5520–5531 *Nucleic Acids Research, 2007, Vol. 35, No. 16* *Published online 17 August 2007*
doi:10.1093/nar/gkm573

Tup1-Ssn6 and Swi-Snf remodelling activities influence long-range chromatin organization upstream of the yeast *SUC2* gene

Alastair B. Fleming[1,2] and Sari Pennings[1,3,*]

[1]Department of Biomedical Sciences, University of Edinburgh, Edinburgh, EH8 9XD, UK, [2]Department of Molecular Genetics and Microbiology, University of New Mexico School of Medicine, 915 Camino de Salud, Albuquerque, New Mexico 87131, USA and [3]Queen's Medical Research Institute, University of Edinburgh, Edinburgh, EH16 4TJ, UK

Received March 30, 2007; Revised June 30, 2007; Accepted July 13, 2007

ABSTRACT

The traditional model for chromatin remodelling during transcription has focused upon the remodelling of nucleosomes at gene promoters. However, in this study, we have determined that Tup1-Ssn6 and Swi-Snf chromatin remodelling activities extend far upstream of the *SUC2* gene promoter into the intergenic region of the *Saccharomyces cerevisiae* chromosome. We mapped the nucleosomal array over a 7.5 kb region that encompassed the *SUC2* gene promoter and upstream region but was devoid of other transcriptionally active genes. Nucleosome positioning over this region was determined under conditions of glucose repression and derepression, and in *snf2*, *ssn6* and *snf2 ssn6* mutant strains. A map detailing remodelling events extending as much as 5 kb upstream of the *SUC2* gene promoter underlines the roles of the Tup1-Ssn6 and Swi-Snf complexes in respectively organizing and disrupting nucleosome arrays. The gene specificity of these events suggests a role in gene regulation. We propose that long-range chromatin remodelling activities of Swi-Snf and Tup1-Ssn6 may ultimately influence whether the chromosomal state of the *SUC2* gene is proficient for transcription. These data raise the possibility that remodelling of extensive chromatin domains may be a general property of the Swi-Snf and Tup1-Ssn6 complexes.

INTRODUCTION

The discovery of chromatin remodelling has revolutionized chromatin research by providing new insights into how the packaging of the eukaryotic genome into nucleosomes participates in gene regulation. Instead of being a static structure, chromatin is now accepted to have a dynamic organization from the nucleosomal level up to higher order structures (1). The identification of numerous multiprotein complexes that are involved in histone modification and remodelling of nucleosome arrays has revealed previously unappreciated levels of control over the basic chromatin organization, with defects in these processes leading to inappropriate gene expression and disease. To understand the dynamic mechanisms that generate these specialized chromatin structures and predispose genes to activation or repression, we have focused on the Tup1-Ssn6 co-repressor and the Swi-Snf co-activator whose interplay regulates the balance between repressed and active chromatin structures at a number of yeast genes.

Swi-Snf is arguably the best-known example of a chromatin remodelling complex that can act as a transcriptional co-activator (2). This large multi-subunit complex is targeted to gene promoters by sequence-specific DNA-binding transcription factors that interact with the Snf5 and Swi1 subunits (3,4). Swi-Snf utilizes the energy from ATP hydrolysis to alter the structure of chromatin, thereby enhancing nucleosomal DNA accessibility and enabling gene transcription (5–9). Potential mechanisms of action include local DNA deformation resulting in nucleosome sliding, and histone octamer transfer in *cis* and in *trans* (10–13). Conversely, the Tup1-Ssn6 co-repressor complex has been shown to organize chromatin into a repressive structure, possibly through direct contact with hypoacetylated histones, and in conjunction with histone deacetylases (14–20). The subsets of genes regulated by these complexes overlap at the *FLO1*, *SUC2* and *RNR3* genes (21–23). Indeed, these genes represent a paradigm for chromatin-mediated gene regulation and offer a unique insight into the interplay between the two complexes.

The traditional model for chromatin remodelling complexes has focused on their activity at gene

*To whom correspondence should be addressed. Tel: +44 131 242 6145; Fax: +44 131 242 6782; Email: Sari.Pennings@ed.ac.uk

promoters (22,24–26). However, evidence is emerging that remodelling also involves longer-range effects. We have shown that remodelling by Swi-Snf, as well as by Tup1-Ssn6, extends some distance upstream of the *FLO1* gene promoter (21). Long-range remodelling has also been shown to occur over the coding regions of genes. For example, Tup1-Ssn6 and Isw2 cooperate to position a regular array of nucleosomes over the promoter and gene-coding region of the repressed *RNR3* gene (27). Upon *RNR3* induction, Swi-Snf is required to disrupt this array (23). Long-range remodelling by Swi-Snf and Isw1 has also been observed at the *HIS3* gene in a mini chromosome context, where induction of transcription was accompanied by the disruption of nucleosomes over the entire gene sequence and flanking regions (28,29). An episomal yeast *CUP1* gene has also been shown to be subject to extensive chromatin remodelling over the entire open reading frame (ORF), 5′ and 3′ flanking regions following activation (30). In each of the above examples, the data suggests that remodelling is a pre-requisite for transcription, and not a consequence of it.

In this study, we have characterized in detail the nature and precise extent of chromatin remodelling in the region upstream of the yeast *SUC2* gene. Using indirect end-labelling and primer extension analyses, we have mapped remodelling events attributable to both Swi-Snf and Tup1-Ssn6 over a 7.5 kb region covering the *SUC2* promoter and far upstream sequences. This extensive nucleosome map reveals how remodelling by both complexes extends as much as 5 kb upstream of *SUC2*. The long-range chromatin remodelling activities reported here support the proposition that it is a general mechanism used by chromatin remodelling complexes such as Swi-Snf and Tup1-Ssn6 to organize extensive chromatin domains in response to cues for transcriptional activation and repression.

MATERIALS AND METHODS

Yeast strains and media

The yeast strains used were wild-type (wt), AFH41 [S288C *MAT*a *ade2-101 his3Δ200 leu2-3,112 lys2-801 trp1Δ901 ura3-52 GAL thr- tyr- arg4-1 hhf1Δ*::HIS3 *hhf2Δ*::LEU2/pUK499 (*URA3*/*HHF2*)]; and its derivatives *snf2*, AFH44 (AFH41 *snf2Δ::TRP1*); *ssn6*, AFH47 (AFH41 *ssn6Δ::kanMX4*) and *snf2 ssn6*, AFH410 (AFH44 *ssn6Δ::kanMX4*) (21). Yeast were grown in YP supplemented with glucose (2%) to mid-log phase. The cultures were divided into two equal portions and harvested by centrifugation. Cell pellets were washed twice in sterile water and resuspended to the same cell density in fresh YP containing glucose at either 2% (repressed, R) or 0.05% (derepressed, D) (22). The cultures were incubated for a further 120 min at 30°C and harvested for either RNA or nuclei preparation.

Chromatin structure analysis

Indirect end-labelling and primer extension analysis were performed as described (21). For the preparation of glucose-repressed nuclei, repression was maintained by supplementing all buffers with 2% glucose (22). For indirect end-labelling, HindIII-digested DNA was probed with PCR fragments corresponding to base-pairs −1099 to −817, −4215 to −3948 and −7801 to −7519 upstream of the *SUC2* ATG (*SUC2* SGD ID: S000001424); DraI-, HinfI- and BamHI-digested DNAs were probed with fragments −1736 to −1359, +1 to +285 and −4033 to −4303, respectively and BsrBI-digested DNAs were probed with fragments −2324 to −1899 and −2697 to −2399.

For primer extension analysis the primers used correspond to positions −797 to −772 (P1); −3155 to −3131 (P2) and −3587 to −3563 (P3) of the *SUC2* upstream sequence. Band intensities were determined by phosphoimager analysis (FujiFilm FLA2000 FluoroImager).

Northern blot analysis

Total RNA was extracted from cells grown as described above and 20 μg samples were analysed by northern blot after electrophoresis in a 1.25% agarose-formaldehyde gel (21). *SUC2*, *ACT1*, *YIL167w*, *YIL166c*, *YIL165c* and *NIT1* transcripts were analysed with probes corresponding to ORF positions +119 to +1222, +411 to +1421, +26 to +620, +598 to +920, +39 to +351 and +47 to +388, respectively.

RT-PCR analysis

Total RNA was treated with DNaseI (Promega) and cDNA was generated using a poly-dT primer and Superscript III reverse transcriptase (Invitrogen). Real time PCRs for *ACT1* and *SUC2* were performed with 1/25 dilutions of the cDNA reactions using the SYBR Green Master Mix (SuperArray) in an ABI 9700 PCR machine. RT-PCRs for *YIL166w*, *YIL165c* and *NIT1* cDNAs were performed on a 1/5 cDNA dilution, and undiluted cDNA reactions. Values were normalized to *ACT1* RNA. Real time PCRs were performed in triplicate. The primer sequences used were: *SUC2*, 5′-CCATTGCTATCGCTCC CAAG-3′ and 5′-TGGAGCCAGAGAAAGCACCT-3′; *ACT1*, 5′-GAGGTTGCTGCTTTGGTTATTGA-3′ and 5′-ACCGGCTTTACACATACCAGAAC-3′; *NIT1*, 5′-T CCCAGAAGCCACTCTTGGT-3′ and 5′-AAACCCCA AAGTTCGATCCC-3′; *YIL165c*, 5′-GCTCGCTTTGA TCTTGACCC-3′ and 5′-TGGAAGACATCTCCCCTAG CA -3′; *YIL166c*, 5′- ACTACCCGGCAATCTGCTGT-3′ and 5′-GGAATGACCCTTTCTGGACCA-3′.

RESULTS

Regulation of *SUC2* and upstream gene transcription

The *SUC2* gene encodes the enzyme invertase required for sucrose utilization and is subject to glucose repression through the Tup1-Ssn6 complex (31,32). As previously shown, transferring cells grown at high glucose concentration (repressing, R) to low glucose conditions (derepressing, D) induces *SUC2* transcription (Figure 1B, lanes 1, 2 and 1C) and a deletion mutation of *SNF2* that cripples the remodelling activity of the Swi-Snf complex, abolishes this induction demonstrating Swi-Snf dependence (Figure 1B,

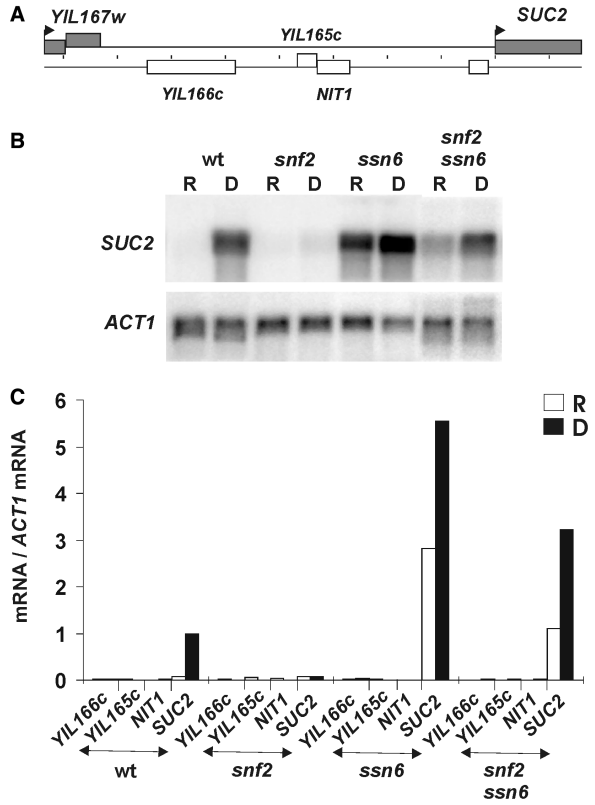

Figure 1. Regulation of *SUC2* and upstream ORF transcription. (**A**) Schematic representation showing the proximity of *SUC2* to upstream transcriptionally inactive (white boxes) and active (grey boxes) ORFs. *YIL167w* is the nearest transcriptionally active gene upstream of *SUC2* and is independent of Swi-Snf and Tup1-Ssn6 regulation. A 1 kb-incremented scale is shown. (**B**) Northern blot analysis of *SUC2* mRNA in wt, *snf2*, *ssn6* and *snf2 ssn6* cells grown under repressing (R) or derepressing (D) conditions. The blot was reprobed with *ACT1* as a loading control. (**C**) RT-PCR analysis of transcription of the *SUC2* gene and upstream ORFs. *YIL166c*, *YIL165c* and *NIT1* are not significantly transcribed in wt or any of the mutant strains grown in repressing (white bars) or derepressing (black bars) conditions. Values are normalized to wt derepressed *SUC2* levels.

lanes 3, 4 and 1C) (31,33). Conversely, deletion of either *SSN6* (Figure 1B, lanes 5, 6 and 1C) or *TUP1* (data not shown) results in high-level constitutive *SUC2* transcription (22,33–35). In the absence of both the Swi-Snf and Tup1-Ssn6 complexes, *SUC2* is also constitutively transcribed, but at lower levels (Figure 1B, lanes 7, 8 and 1C) (22,33,34).

Numerous studies had suggested that upon gene activation or repression chromatin remodelling is limited to the immediate promoter region. However, evidence is emerging that remodelling complexes can in fact operate over longer distances. Indeed, our previous work indicated that this was the case for Swi-Snf and Tup1-Ssn6 regulation of *FLO1* transcription (21). If similar long-range remodelling were apparent far upstream of *SUC2*, it would strengthen the case that the ability to organize extensive chromatin domains is a general feature of Swi-Snf and Tup1-Ssn6. However, prior to embarking upon an analysis of chromatin remodelling events upstream of *SUC2*, we first characterized the extent of distal gene activity potentially affecting this region.

SUC2 is located ~35 kb from the telomere on the left arm of chromosome IX (36). Four ORFs are located in the 10 kb region upstream of *SUC2*. Two ORFs (*YIL167/168w* and *YIL 164/165c*) are interrupted by a stop codon in S288C strains, while the short *YIL163c* has dubious ORF status (Figure 1A). We analysed these ORFs for transcriptional activity, and determined whether they were subject to regulation by Tup1-Ssn6 or Swi-Snf. From northern blot analysis, only the far upstream ORF *YIL167w* yielded a detectable transcript, and this was unaffected in any of the mutant backgrounds under conditions of glucose repression and derepression (data not shown). Further analysis of the remaining genes by quantitative RT-PCR detected no significant transcription (Figure 1C). We therefore chose the 3′ end of the *YIL167w* ORF as the upstream boundary for our mapping analysis. This provided a transcriptionally 'quiet' region spanning 7.5 kb upstream of *SUC2* in which to identify chromatin remodelling effects specific to Swi-Snf and Tup1-Ssn6 that could be attributed to *SUC2* without interference from neighbouring gene transcription.

Mapping nucleosome positions at the *SUC2* promoter and upstream region

We used micrococcal nuclease (MNase) digestion and the methods of indirect end-labelling and primer extension analysis to determine nucleosome positions at the upstream *SUC2* chromosomal locus (37). These methods detect translationally positioned nucleosomes by virtue of the protection they afford to nucleosomal DNA against MNase digestion. Nucleosomes are allocated to ~145 bp regions of protection between strong cut sites in the chromatin cleavage pattern as compared with the corresponding region of digestion in the naked DNA.

We mapped 7.5 kb of nucleosome array upstream of the derepressed *SUC2* gene in a variety of strain backgrounds in order to distinguish the effects of different chromatin remodelling activities. Chromatin from *ssn6* and *snf2* deletion strains revealed remodelling in the absence of the Tup1-Ssn6 and Swi-Snf complexes, respectively. Because these remodelling events could directly reflect the absence of a particular remodelling complex, or the unmasking of underlying activities of the other complex, the *ssn6 snf2* double deletion strain was also included in our analyses to distinguish this. Chromatin from wild-type (wt), *ssn6*, *snf2* and *ssn6 snf2* nuclei was characterized under glucose derepressed conditions, in which only the *snf2* strain does not express *SUC2*. To reveal the full impact on the upstream chromatin resulting from Tup1-Ssn6 repression of the *SUC2* gene, we additionally mapped nucleosome positions in a wt strain grown under glucose repressed conditions. Finally, the corresponding 7.5 kb naked DNA control pattern of MNase cutting allowed us to unequivocally identify the sites of nucleosomal protection in the chromatin patterns and to assign nucleosome positions.

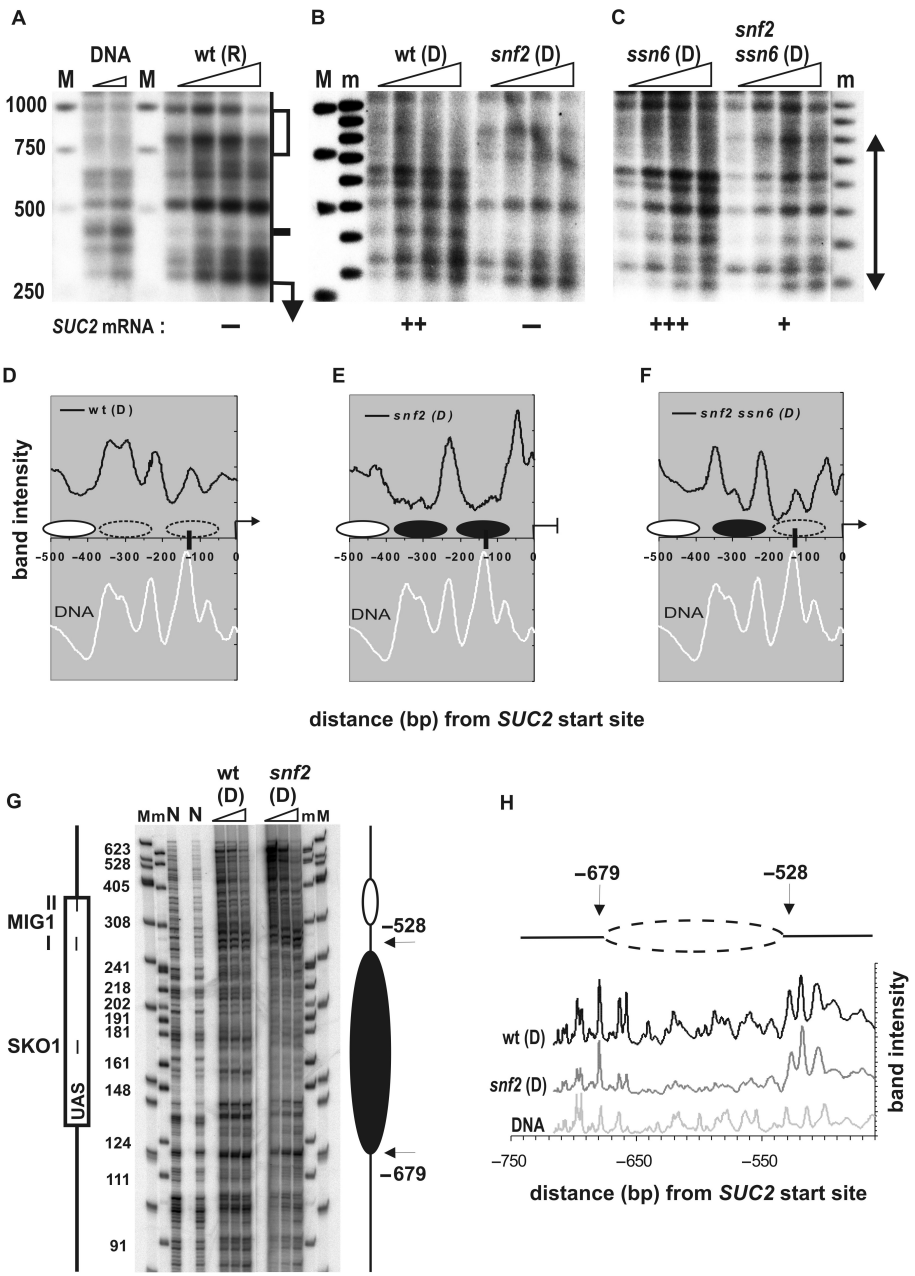

Figure 2. Mapping chromatin remodelling at the *SUC2* promoter. (**A–C**) Indirect end-labelling analysis of MNase cleavage sites in chromatin from wt repressed (R) and derepressed (D) wt, *snf2*, *ssn6* and *snf2 ssn6* strains at the *SUC2* promoter relative to a HinfI site (+292 bp). Naked DNA digests (DNA), 100 bp (m) and 1 kb (M) molecular weight markers are indicated. The positions of the *SUC2* UAS (white box), TATA box (thin black box) and the coding region start site (ATG/+1; hooked arrow) are indicated in A. Presence (+) or absence (−) of *SUC2* transcription is labelled below each blot. The double-headed arrow indicates the region of the gel for which phosphoimager traces are shown in D–F. The full-length blot is shown in Supplementary Figure S1. (**D–F**) Phosphoimager scans of the third lane of the indicated digests in A–C were plotted on a linear base-pair scale relative to the *SUC2* ATG (+1), and nucleosomes allocated. The gel migration distances in each trace were recalculated to base-pairs, using the equation for the DNA standard curve determined by polynomial regression analysis of the bands from the molecular weight markers. Nucleosome core particles were allocated to regions of 145 bp centered on minima between strong cut sites in the MNase chromatin cutting pattern where such minima were absent in the DNA pattern or contained peaks not found in chromatin. Nucleosomes that were remodelled (dashed ovals), or repositioned as compared to wt derepressed chromatin (black ovals) are indicated. White ovals indicate uncertain nucleosome positions where the DNA and chromatin patterns were similar. (**G**) High resolution primer extension analysis of Swi-Snf-dependent chromatin remodelling at the *SUC2* UAS from a primer starting at −797 bp (P3), and corresponding phosphoimage scans (**H**). The location of the UAS (white box) and of the Sko1- and two Mig1-binding sites (I and II) are shown. Markers are a 5′ end-labelled Φx174 HinfI digest (M) and a 3′ filled-in pBR322 MspI digest (m). Nucleosome positions in *snf2* chromatin are depicted beside the gels, as described above. Arrows indicate major cleavage sites and the numbers correspond to their distance (bp) from the A of the initiation codon of *SUC2*. The nucleosome remodelled by Swi-Snf in wt (D) chromatin is depicted as a dashed oval above the phosphoimage scans.

Multiple short-range maps were required to cover the full 7.5 kb region (Figures 2–5). In all regions where mapping was performed from both upstream and downstream restriction sites, the data were consistent. Densitometry traces from each analysis were linearized and combined to produce the composite map of the upstream *SUC2* region that is shown in Figure 6.

Tup1-Ssn6 is required to position a nucleosome at the glucose-repressed *SUC2* TATA box

Our data confirm previous studies demonstrating chromatin remodelling at the *SUC2* promoter upon glucose derepression in wt cells. Here, strongly positioned nucleosomes in repressed chromatin that occlude the *SUC2* TATA box and upstream activating sequence (UAS) revert to a naked DNA pattern in derepressed chromatin [TATA box: Figure 2A, B and D, compare wt (R) with wt (D) and DNA; UAS: Figure 2G and H, compare wt (D) with DNA (N)] (38–40). The remodelling of these nucleosomes on the proximal *SUC2* promoter was attributed to the Swi-Snf complex because this remodelling was absent in *snf2* derepressed chromatin [Figure 2B, E and G, H; compare wt (D) and *snf2* (D)] (22,41–43). Under repressing conditions, Tup1-Ssn6 is recruited to the proximal *SUC2* promoter by the DNA-bound Mig1p, Nrg1 and Sko1 repressors in response to signal transduction pathways (44,45). In glucose derepressed *ssn6* chromatin, we confirm the remodelling of the nucleosome that occludes the TATA box in wt repressed chromatin (Figure 2C) (22,40). Our analysis of *snf2 ssn6* derepressed chromatin at the *SUC2* TATA box also shows that this remodelling occurs even in the absence of Swi-Snf (and Tup1-Ssn6) [Figure 2C and F, compare *ssn6* (D) to *snf2 ssn6* (D)] (22,40). These data are consistent with the suggestion that factors other than Swi-Snf may be involved in the remodelling of this nucleosome in the absence of Tup1-Ssn6 (22). However, an alternative interpretation is that the presence of the positioned nucleosome at the TATA box is dependent on dominance of the Tup1-Ssn6 complex (as in wt repressed and *snf2* chromatin), rather than its removal being dependent on the Swi-Snf complex. This would imply a default active chromatin pattern in the absence of both remodelling complexes, matching the *SUC2* gene activity in the *snf2 ssn6* double deletion mutant.

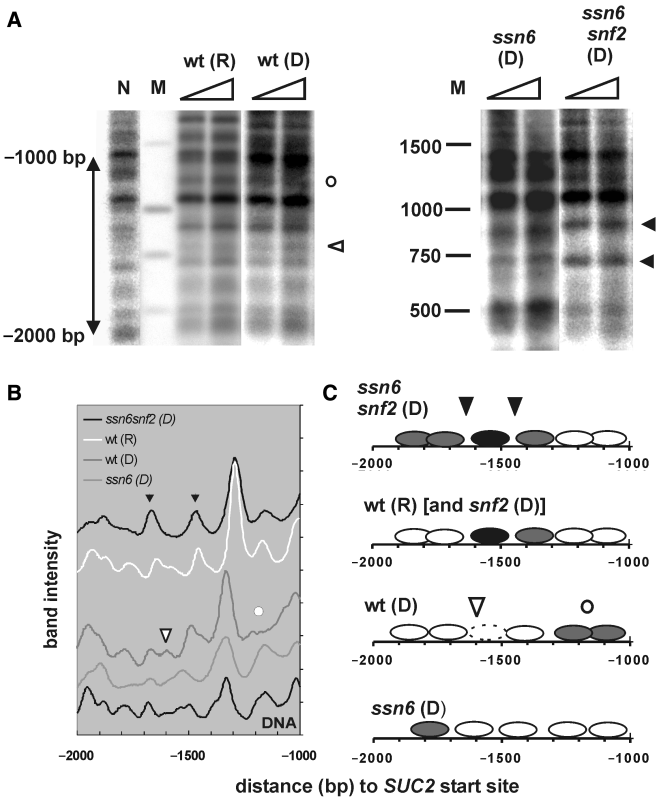

Figure 3. Mapping Swi-Snf chromatin remodelling 1.6 kb upstream of *SUC2*. (**A**) Indirect end-labelling analysis of MNase cleavage sites relative to a BsrBI site (−2375 bp). Legend details are as described for Figure 2. White and black arrowheads denote enhanced digestion in wt (D) and *ssn6 snf2* (D) chromatin, respectively as described in text. The white circle indicates protection from digestion in wt (D) chromatin at −1200 bp. The full-length blot is shown in Supplementary Figure S2. (**B**) Phosphoimager scans of the second lane of each digest in A were plotted on a linear base-pair scale relative to the *SUC2* ATG (+1). (**C**) Allocation of nucleosome positions from the phosphoimage traces shown in B, highlighting two strong cut sites (black arrowheads) in *snf2 ssn6* (D) chromatin that indicate the presence of a strongly positioned nucleosome (black oval). Grey ovals indicate nucleosome positions offering 145 bp protection of digestion in chromatin as compared to a corresponding region of digestion in naked DNA; white ovals are uncertain nucleosome positions. Black ovals depict positioned nucleosomes that contrast to the wt (D) chromatin that is sensitive to digestion at this site (white arrowhead). The Swi-Snf remodelled nucleosome in wt (D) chromatin is depicted as a dashed oval. The white circle is as described in A.

Swi-Snf-dependent chromatin remodelling 1.6 kb upstream of *SUC2*

As we mapped chromatin further upstream from the *SUC2* promoter, we identified two strong MNase cut sites in derepressed *snf2 ssn6* chromatin that indicated the presence of a positioned nucleosome at around −1600 bp [*snf2 ssn6* (D): Figure 3A, B (black gel trace) and C; the two black arrowheads denote the strong cut sites, and the black oval indicates the corresponding positioned nucleosome]. A similar but less distinct pattern was present in wt repressed [wt (R): Figure 3A, B (white gel trace) and C] and derepressed *snf2* chromatin (data not shown, see gel trace in Figure 6). However, in derepressed wt chromatin, digestion between these cut sites at −1600 bp indicated the loss of nucleosomal protection in this region [wt (D): Figure 3A, B (upper grey trace) and C; white arrowhead indicates digestion at −1600 bp, and the dashed oval signifies a remodelled nucleosome at this site as compared to *snf2 ssn6* (D) and wt (R) chromatin]. This remodelling event is attributable to Swi-Snf, since in the absence of this complex (*snf2* deletion) the nucleosome was reinstated. In derepressed *ssn6* chromatin, a digestion pattern equivalent to naked DNA was observed [Figure 3B, compare *ssn6* (D) lower grey trace to black DNA trace], which was also linked to the presence of the Swi-Snf complex since its absence (*snf2 ssn6* deletion) again reinstated the nucleosomal pattern. In *ssn6* chromatin, the naked DNA-like cutting

pattern continued from this point onward towards the coding region over a distance of at least 1500 bp. In contrast, a well-defined nucleosomal array was present in wt repressed chromatin. This was particularly noticeable when the repressed and derepressed wt digests were electrophoresed side by side as bands are narrower and more distinct in wt repressed chromatin [Figure 3A, compare wt (R) and wt (D)]. Derepressed wild-type and *snf2* chromatin showed hybrid traces, where some nucleosome boundaries were preserved and others were lost. Most notably, a boundary at −1200 bp is clearly absent in derepressed wt chromatin [wt (D): Figure 3A, B (upper grey trace) and C; white circle denotes protection from digestion at this site as compared to wt (R) chromatin]. Overall, the data suggests Swi-Snf dependent remodelling dominates this chromatin region following *SUC2* induction.

Tup1-Ssn6 antagonism of Swi-Snf remodelling activity determines nucleosome positioning at the 3.3 kb upstream region

Chromatin remodelling was also observed ~3.3 kb upstream of the *SUC2* coding region. In wt repressed chromatin, a pattern distinct from the naked DNA control indicated the presence of nucleosomes in this region [Figure 4A and B, compare wt (R) to DNA]. The pattern included a cut site at −3400 bp that was weak or not observed in *snf2* or *ssn6* derepressed chromatin, and which most likely represents a DNA region between two positioned nucleosomes (Figure 4A–C, black arrowhead). Protection of a cut site apparent in naked DNA and the *snf2* and *ssn6* derepressed chromatin was also evident in the wt repressed strain at −3300 bp (Figure 4A and B, white arrowhead), indicating a positioned nucleosome at this region [Figure 4C, wt (R), black oval]. In derepressed wt chromatin, a diffuse cutting pattern was indicative of a less precisely positioned nucleosome occupying this region [data not shown, see wt (D) gel trace in Figure 6]. This pattern persisted in derepressed *snf2* chromatin, suggesting that the remodelling is Swi-Snf-independent [Figure 4A, *snf2* (D), 4B (white trace) and 4C (overlapping white ovals)]. By contrast, in derepressed *ssn6* chromatin, the cleavage pattern was similar to that seen in naked DNA [Figure 4A, B (compare the grey trace to lowermost black trace) and C]. However, when *snf2* was also deleted in the *ssn6* mutant (data not shown, see *snf2 ssn6* trace in Figure 6), the pattern reverted to that seen in the derepressed wt chromatin, suggesting that Swi-Snf remodels this nucleosome, but only in the absence of Tup1-Ssn6. Therefore, it appears to be the balance between the positioning activity of Tup1-Ssn6 and the remodelling activity of Swi-Snf that determines the position of this particular nucleosome upon *SUC2* activation.

High resolution analysis of the −3500 to −3200 region by primer extension confirmed the naked DNA-like pattern in the absence of Tup1-Ssn6, confirming nucleosome remodelling at this site [Figure 4D and E, compare *ssn6* (D) to DNA (N)]. Furthermore, by superimposing the indirect end-labelling cleavage patterns (Figure 4E, white traces) onto the primer extension cleavage patterns (Figure 4E, black traces), the data from the two techniques show a strong correlation. This also validates the accuracy of the lower-resolution but longer-range indirect end-labelling nucleosome mapping method used primarily in this study.

A further instance of remodelling was detected at −2900 bp, where a strong cut site between two positioned nucleosomes was present in the chromatin of all strains but much weaker in derepressed *ssn6* chromatin (Figure 4A, white circle). As enhanced cutting at −2900 bp was restored in *snf2 ssn6* chromatin, the Swi-Snf complex appears responsible for this effect.

Swi-Snf remodels two nucleosomes 5 kb upstream of *SUC2*

Proceeding more distally from the *SUC2* promoter, a further instance of remodelling was suggested at −4800 bp, signified by a wide peak of increased cutting in derepressed *ssn6* chromatin (Figure 5A, black arrowhead and Supplementary Figure S4). In derepressed *snf2 ssn6* chromatin, however, protection from digestion at this site was compatible with the presence of a nucleosome, suggesting Swi-Snf was responsible for the subtle remodelling observed in *ssn6* chromatin (Figure 5A, compare black and white traces). To confirm a role for Swi-Snf in remodelling at this site, we analysed the region in greater detail by indirect end-labelling analysis from a BamH1 restriction site present ~800 bp upstream of the putative remodelled nucleosome (Figure 5B and Supplementary Figure S5). In derepressed wt chromatin, nucleosomal protection was weaker at −4800 bp and appeared as a shoulder (Figure 5B, black arrowhead, black trace), similar to that observed in *ssn6* chromatin, and additional enhanced cutting was also visible at a site −5300 bp upstream of *SUC2* (Figure 5B, white arrowhead). This enhanced cutting was not evident in the repressed wt or derepressed *snf2* chromatin patterns (Figure 5B, grey and white traces) and is compatible with a labile nucleosome being displaced in derepressed wt chromatin or in the absence of *ssn6*. This remodelling event is dependent on the Swi-Snf complex, as deletion of *snf2* restored the positioned nucleosome.

Chromatin remodelling cannot be detected over the 2 kb region furthest upstream of *SUC2*

As we mapped nucleosome positions from −5500 bp upstream of *SUC2* towards the transcriptionally active ORF *YIL167w*, which formed the 7.5 kb upstream boundary of our mapping analysis, we found over 2 kb of chromatin organized into a very regular array of nucleosomes (Figure 6 and Supplementary Figure S6). The positions of 12 nucleosomes were easily distinguished by comparison with the naked DNA trace. Significantly, no differences could be detected between different strain backgrounds as the MNase cutting patterns were essentially superimposable. This argues against the occurrence of randomly distributed chromatin remodelling events in the various yeast mutants. Thus, chromatin remodelling activity does not extend further than 5.5 kb upstream of *SUC2*.

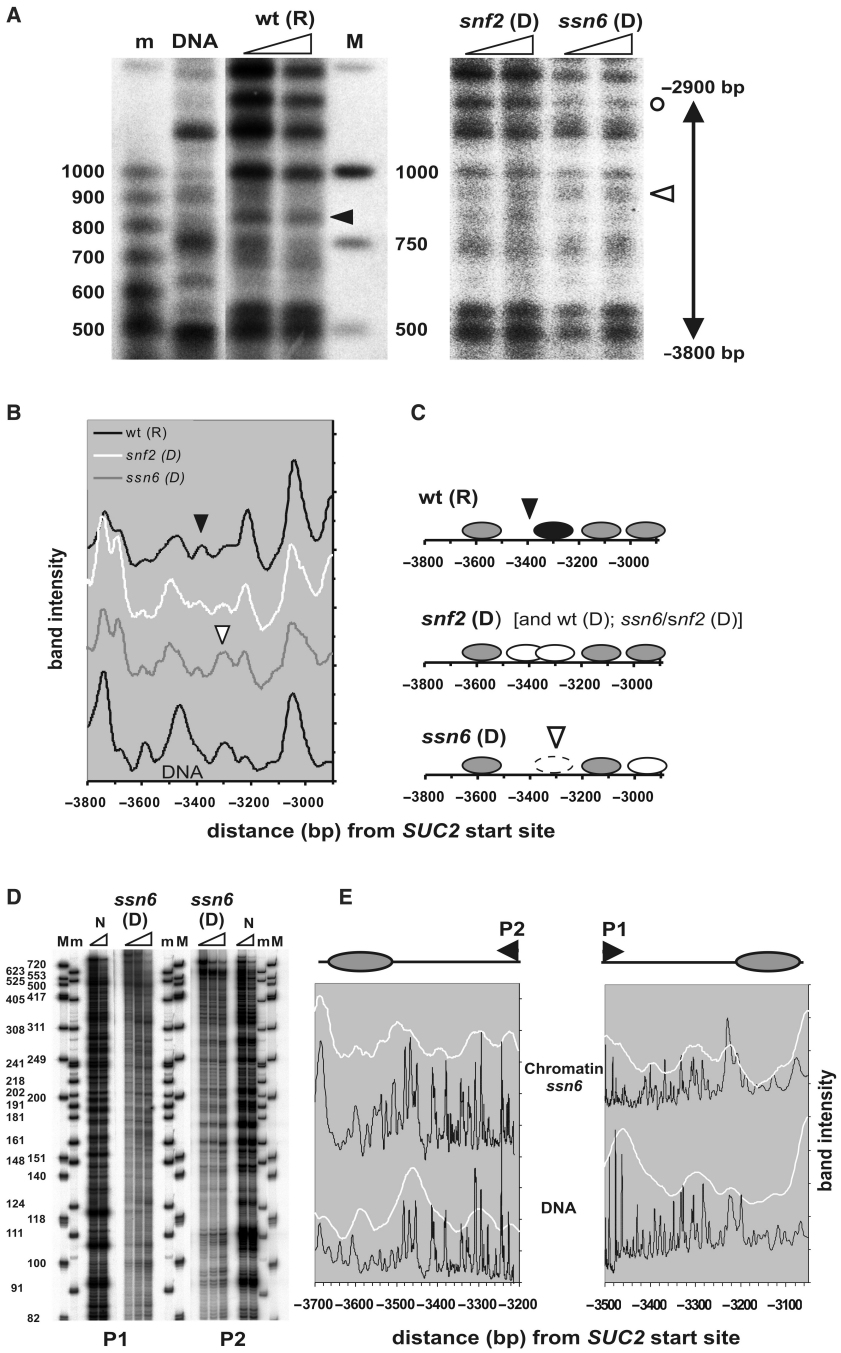

Figure 4. Mapping antagonistic chromatin remodelling activity 3.3 kb upstream of *SUC2*. (**A**) Indirect end-labelling analysis of MNase cleavage sites relative to a HindIII site (−4220 bp). The legend is as described for Figures 2 and 3. Significant cut sites in the wt (R) and *ssn6* (D) chromatin are indicated with black and white arrowheads, respectively. The white circle denotes protection from digestion in *ssn6* (D) chromatin at −2900 bp. The full-length blot is shown in Supplementary Figure S3. (**B**) Phosphoimager scans of the first lane of each digest in A plotted on a linear base-pair scale relative to the *SUC2* ATG (+1). (**C**) Allocation of nucleosome positions from the phosphoimage traces shown in B. Swi-Snf-independent nucleosome mobility [*snf2* (D), overlapping white ovals] at −3300 to −3400 bp is indicated. The positioned nucleosome in wt (R) chromatin is depicted as a black oval. Swi-Snf remodelling activity generates a naked DNA-like pattern in the absence of Tup1-Ssn6 under conditions of derepression [*ssn6* (D), dashed oval]. (**D**) High resolution primer extension analysis of MNase cleavage sites in derepressed *ssn6* chromatin from primers starting at −3131 (P1) and −3587 bp (P2). (**E**) Gel traces of *ssn6* (D) chromatin and naked DNA digests shown in D were plotted (black traces) on a linear base-pair scale. The corresponding gel traces from the indirect end-labelling analysis in B are plotted (white traces) for comparison; alignment with the high resolution trace was within 20 bp. The primers used for the gels in D are depicted as arrowheads P1 and P2, and putative nucleosome positions are depicted as grey ovals.

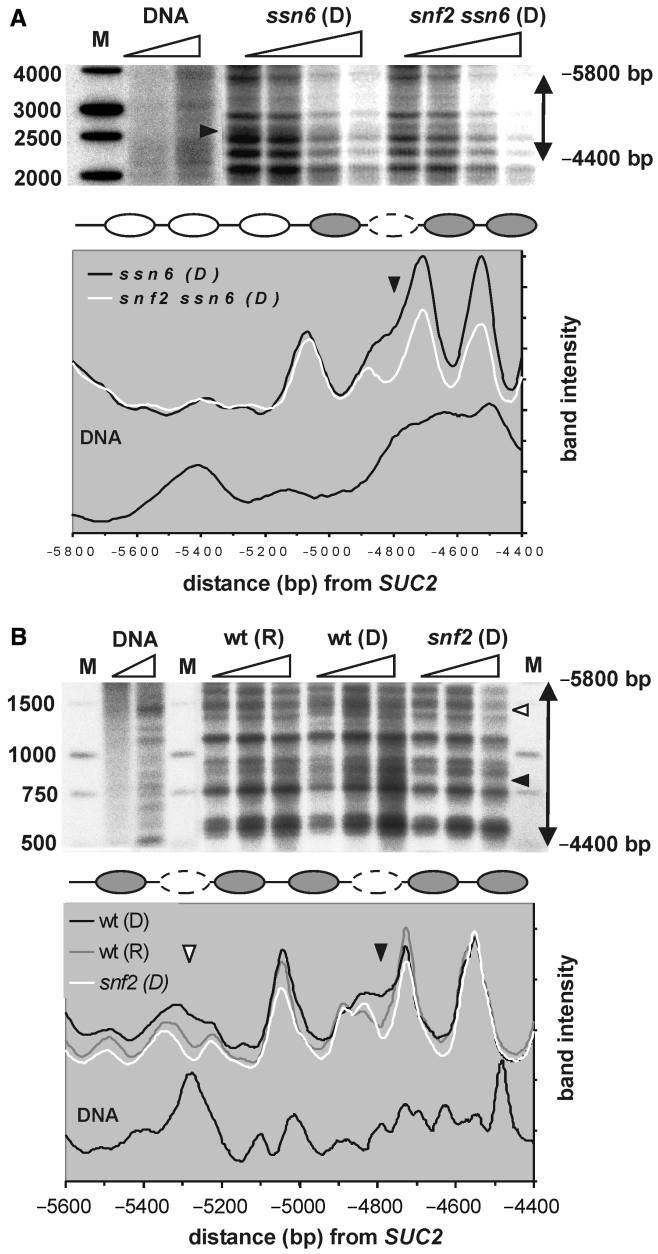

Figure 5. Mapping Swi-Snf-dependent chromatin remodelling 5 kb upstream of *SUC2*. (**A**) Indirect end-labelling analysis of MNase cleavage sites relative to a BsrBI site (−2375 bp) and corresponding phosphoimage scans in *ssn6* and *snf2 ssn6* mutant chromatin from cells grown under derepressing (D) conditions. The black arrowhead indicates enhanced cleavage in *ssn6* chromatin at −4800 bp. For legend details see Figures 2 and 3. For the full-length blot refer to Supplementary Figure S4. (**B**) Indirect end-labelling analysis of MNase cleavage sites relative to a BamHI site (−4014 bp) and corresponding phosphoimage scans confirm Swi-Snf remodelling in wt derepressed (D) chromatin at −4800 and at −5300 bp (black and white arrowheads denote enhanced cleavage in wt derepressed chromatin at −4800 and −5300 bp, respectively). The full-length blot is shown in Supplementary Figure S5.

DISCUSSION

We have detected and characterized long-range chromatin remodelling by Swi-Snf and Tup1-Ssn6 in the extended *SUC2* upstream region following glucose derepression. The *SUC2* gene is specifically induced by low glucose within a 7.5 kb region free of other transcriptional activity. Our results, summarized in Figure 6, suggest that chromatin remodelling extends far beyond what is generally considered the *SUC2* promoter region, with the most distant event detected at −4800 bp. Other remodelling events occur at −3300, −2900, −1500, −1100, −500 and −120 bp. Significantly, no instances of remodelling were observed within the ~2.5 kb of chromatin analysed upstream of this region. This suggests that the characterized long-range chromatin alterations by the Tup1-Ssn6 and Swi-Snf remodelling complexes are linked to their control of *SUC2* transcription.

Our data confirm previous studies showing chromatin remodelling of nucleosomes at the *SUC2* TATA box and UAS following *SUC2* derepression (22,39). However, the observation that remodelling at the TATA box is also found in derepressed *snf2 ssn6* chromatin is incompatible with the earlier proposal that the Swi-Snf complex is responsible for this event (40,41,43). Instead, it points to the dependence of the position of this nucleosome on the Tup1-Ssn6 complex. Consistent with this, recent work has shown that Tup1 can regulate Rap1 binding by controlling nucleosome occupancy at some Rap1 binding sites (46). However, the involvement of remodelling complexes other than Swi-Snf in disrupting the *SUC2* array also cannot be discounted (22).

Upstream from the *SUC2* promoter, the less dramatic, but reproducible nucleosome remodelling events in the various strain backgrounds displayed particular characteristics. Thus, instances of remodelling in derepressed *ssn6* chromatin were in most cases reversions to the naked DNA pattern [Figure 6, *ssn6* (D)]; derepressed *snf2* chromatin bore the greatest resemblance to the repressed wt pattern [Figure 6, compare *snf2* (D) and wt (R)]; whereas derepressed *snf2 ssn6* chromatin most resembled wt derepressed chromatin [Figure 6, compare *snf2 ssn6* (D) and wt (D)]. This behaviour parallels the relationship between these strains in terms of activity of the *SUC2* gene (Figure 1B and C). It is also consistent with our observations at the *FLO1* gene, which suggested that the balance between these antagonizing remodelling activities controls the chromatin organization of this gene (21). Hence, depletion of both Tup1-Ssn6 and Swi-Snf has less impact on chromatin structure and gene activity than the absence of a single complex, which mimics the situation where the other complex dominates.

The many apparent reversals to the naked DNA pattern in *ssn6* chromatin indicate nucleosome loss or randomization rather than translational rearrangement of nucleosome positions. Nucleosome loss has been shown for the TATA box of the active *SUC2* gene (47). Near the *SUC2* coding region, the MNase cleavage pattern of naked DNA bears some similarity to the nucleosomal pattern, most likely because the sequence-specificity of the nuclease reveals a biased nucleotide sequence distribution that is occasionally in phase with the nucleosome array, as has been noted for other genes (30,48). This might leave less freedom for the repositioning of nucleosomes, although a randomization or mobilization of nucleosome positions might also resemble a naked DNA pattern. The far

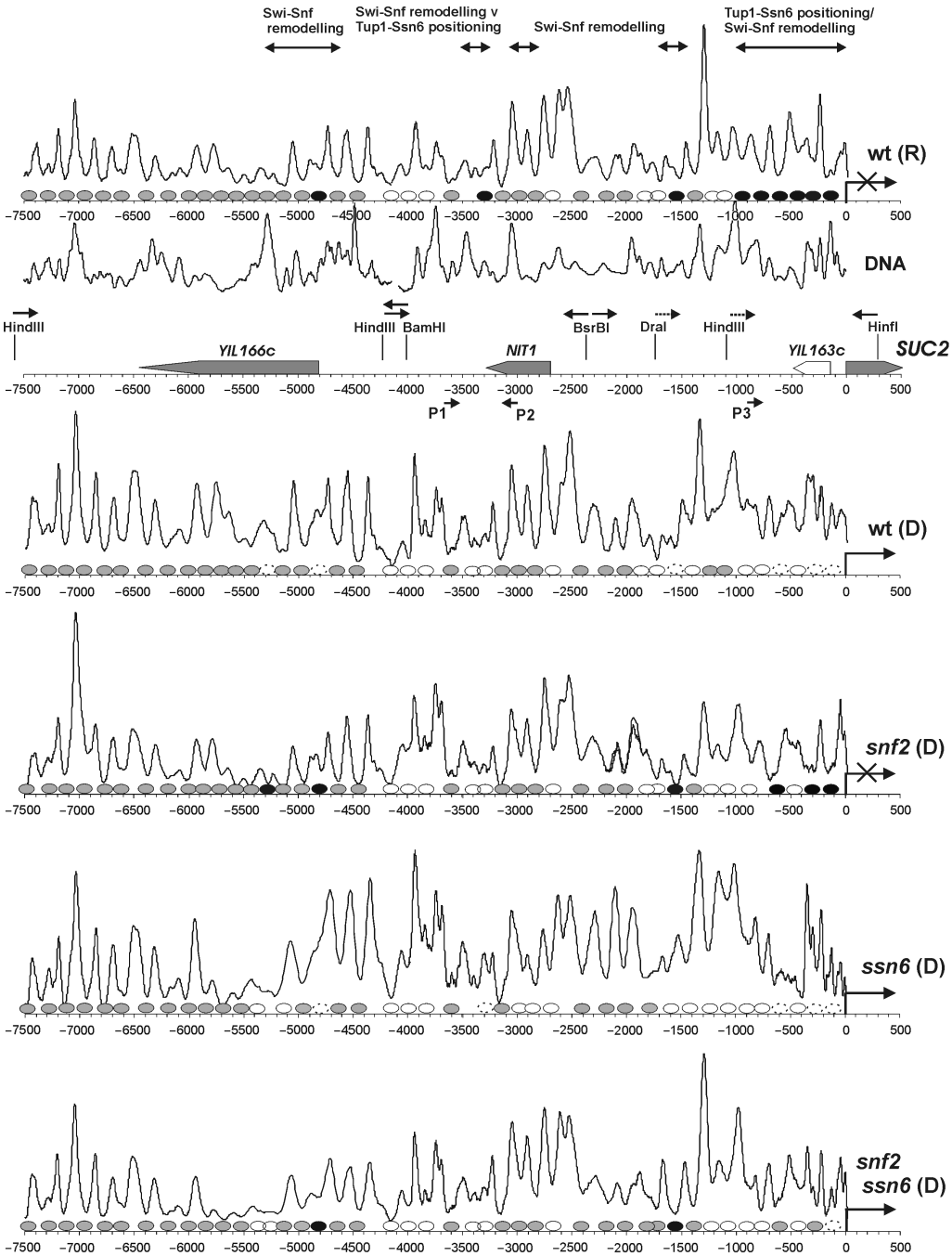

Figure 6. Map of the 7.5 kb region upstream of *SUC2* showing the long-range nucleosome remodelling activities of Swi-Snf and Tup1-Ssn6. Composite map of gel traces to show nucleosome arrays and chromatin remodelling in the strains indicated. Gel migration distances from separate indirect end-labelling analyses were converted to base-pairs as described in Figure 2 and plotted on a linear base-pair scale relative to the *SUC2* ATG (+1). The probes (arrows), and the restriction enzyme sites relative to which indirect end-labelling analyses were performed are shown; dashed arrows indicate probes for which the data were not shown. Primer extension oligonucleotides are indicated (P1, P2 and P3). Grey ovals depict nucleosome core particles of 145 bp centred on minima between strong cut sites in the micrococcal nuclease chromatin cutting pattern where such minima were absent in the DNA pattern or contained peaks not found in chromatin. Where the chromatin and DNA patterns were significantly similar, putative nucleosome positions have been assigned (white ovals). Black ovals depict nucleosomes repositioned in the strain indicated as compared to the wt derepressed array. Remodelled nucleosomes are depicted as dashed ovals. Overlapping ovals indicates imprecisely mapped nucleosome positions. Low band intensities in the −5300 bp region are due to low hybridization signals at the junction of two traces; at other trace junctions, significant overlap between traces compensated for this effect. In the −4100 bp region, the naked DNA traces do not overlap and a nucleosome has been arbitrarily assigned to chromatin at this site. The mapping of the nucleosome array starts at the *SUC2* coding region and extends upstream as far as the end of the *YIL167w* gene. The presence (hooked arrow) and absence (crossed hooked arrow) of transcription from *SUC2* in the different strain backgrounds is indicated. Orientation and position of ORFs (grey boxes) are indicated.

upstream reversals to the naked DNA pattern in derepressed *ssn6* chromatin are due to Swi-Snf activity, since they are not observed in *snf2 ssn6* chromatin [Figure 6, compare *ssn6* (D) and *snf2 ssn6* (D) at −3300 and −4800 bp]. This underlines the roles of the Tup1-Ssn6 and Swi-Snf complexes in respectively organizing and disrupting nucleosome arrays. On this basis, wt repressed and *snf2* chromatin represent the dominant effects of Tup1-Ssn6 on the nucleosome array, and derepressed wild-type [where Tup1 persists (49)] and *ssn6* chromatin represent the dominant role of Swi-Snf. The *snf2 ssn6* chromatin shows that, at the *SUC2* gene, the remodelling complexes operate largely within the framework of an array of nucleosome positions predetermined by the DNA sequence (50–52).

The *SUC2* upstream sequence includes many transcription factor-binding sites, some of which are unique while others are redundant. However, only a fraction of consensus sites are occupied by their respective binding factors, and this restricts our ability to relate individual changes in the nucleosome array to features in the underlying DNA sequence (53,54). For example, the DNA sequence at the −4800 bp Swi-Snf-remodelled site harbours a unique Rox1-binding site. Although Rox1 is known to recruit Tup1-Ssn6 to repress hypoxic genes under aerobic conditions, we do not expect that this site is occupied under our conditions (55).

An important suggestion from our work is that long-range chromatin remodelling may well be a general feature of chromatin modifying complexes such as Tup1-Ssn6 and Swi-Snf. Promoter-centred models of chromatin remodelling reflect the emphasis of gene regulation research on the proximal upstream region of genes. Few studies have investigated the effects of remodelling into intergenic regions. However, it has been found that Swi-Snf-dependent chromatin remodelling extends along the circular chromatin of episomes carrying the *HIS3* gene, including the coding region (28,29). *RNR3* has also been shown to be subject to remodelling over the entire length of the coding region and promoter (27). Furthermore, genome-wide chromatin immunoprecipitation studies have localized the Swi-Snf-related RSC complex at many intergenic locations as well as at promoters (9). Our findings, both at *SUC2* and *FLO1*, indicate that remodelling complexes can indeed function at such intergenic regions, and in a manner that can be correlated to the activity of the genes they control.

Although remodelling of the nucleosome array upstream of *SUC2* by the Tup1-Ssn6 and Swi-Snf complexes is not restricted to the proximal *SUC2* promoter, it does appear to be confined to within several kilobase upstream of this promoter. It is not clear whether this is a consequence of boundary effects (56), or reflects the natural range of direct or indirect nucleosome remodelling effects emanating from a site of complex recruitment, or a distribution of complex-recruitment sites. Nearby genes that are not under the control of these complexes could also conceivably delimit remodelling (57). Although the ORFs in the *SUC2* upstream region are not active under the conditions of this study, their bound factors or histone modification patterns might prevent the propagation of *SUC2*-associated nucleosome remodelling effects (58). Far upstream instances of chromatin remodelling could equally be a direct consequence of the presence of Tup1-Ssn6 and Swi-Snf complexes targeted to these regions in addition to their documented promoter associations (59,60). In support of this model are the observations of Swi-Snf complexes forming loops and controlling the helical tension between attachment sites, and of Tup1-Ssn6 showing a continuous association along the chromatin fibre (12,16,61–63). Alternatively, the remodelling could be at the level of higher order chromatin structure, as has been suggested for Swi-Snf activity (64). Finally, recent observations of nuclear relocation of the *SUC2* gene upon activation or repression suggest possible extensive structural rearrangements (65).

Long-range chromatin remodelling seems at odds with the high gene density in yeast. What are seen at *FLO1*, and here at *SUC2*, may be just two examples demonstrating the potential of these complexes to remodel large domains when the gene under their control is in a less gene-dense region. The dynamic changes to such a large region of chromatin may parallel the extensive range of histone modifications, such as histone acetylation and methylation, that may also be in effect over larger regions of chromatin (66). This regional chromatin organization may provide a background essential for gene regulation to take place, and ultimately determine the accessibility of the promoter.

SUPPLEMENTARY DATA

Supplementary Data are available at NAR Online.

ACKNOWLEDGEMENTS

We gratefully acknowledge Colin Davey, Mary Ann Osley, Michael Pikaart, Cheng-Fu Kao and Chang-Hui Shen for advice and comments on this work, and all members of the Pennings and Osley laboratories for valuable discussions. This work was supported by a Wellcome Senior Research Fellowship to S.P. (045117). Funding to pay the Open Access publication charges for this article was provided by The Wellcome Trust.

Conflict of interest statement. None declared.

REFERENCES

1. Hayes,J.J. and Hansen,J.C. (2001) Nucleosomes and the chromatin fiber. *Curr. Opin. Genet. Dev.*, **11**, 124–129.
2. Sudarsanam,P., Iyer,V.R., Brown,P.O. and Winston,F. (2000) Whole-genome expression analysis of snf/swi mutants of Saccharomyces cerevisiae. *Proc. Natl Acad. Sci. USA*, **97**, 3364–3369.
3. Neely,K.E., Hassan,A.H., Brown,C.E., Howe,L. and Workman,J.L. (2002) Transcription activator interactions with multiple SWI/SNF subunits. *Mol. Cell. Biol.*, **22**, 1615–1625.
4. Prochasson,P., Neely,K.E., Hassan,A.H., Li,B. and Workman,J.L. (2003) Targeting activity is required for SWI/SNF function in vivo and is accomplished through two partially redundant activator-interaction domains. *Mol. Cell*, **12**, 983–990.

5. Imbalzano,A.N., Kwon,H., Green,M.R. and Kingston,R.E. (1994) Facilitated binding of TATA-binding protein to nucleosomal DNA. *Nature*, **370**, 481–485.
6. Kwon,H., Imbalzano,A.N., Khavari,P.A., Kingston,R.E. and Green,M.R. (1994) Nucleosome disruption and enhancement of activator binding by a human SW1/SNF complex. *Nature*, **370**, 477–481.
7. Côté,J., Quinn,J., Workman,J.L. and Peterson,C.L. (1994) Stimulation of GAL4 derivative binding to nucleosomal DNA by the yeast SWI/SNF complex. *Science*, **265**, 53–60.
8. Owen-Hughes,T., Utley,R.T., Côté,J., Peterson,C.L. and Workman,J.L. (1996) Persistent site-specific remodeling of a nucleosome array by transient action of the SWI/SNF complex. *Science*, **273**, 513–516.
9. Becker,P.B. and Hörz,W. (2002) ATP-dependent nucleosome remodeling. *Annu. Rev. Biochem.*, **71**, 247–273.
10. Phelan,M.L., Schnitzler,G.R. and Kingston,R.E. (2000) Octamer transfer and creation of stably remodeled nucleosomes by human SWI-SNF and its isolated ATPases. *Mol. Cell. Biol.*, **20**, 6380–6389.
11. Whitehouse,I., Flaus,A., Cairns,B.R., White,M.F., Workman,J.L. and Owen-Hughes,T. (1999) Nucleosome mobilization catalysed by the yeast SWI/SNF complex. *Nature*, **400**, 784–787.
12. Havas,K., Flaus,A., Phelan,M., Kingston,R., Wade,P.A., Lilley,D.M. and Owen-Hughes,T. (2000) Generation of superhelical torsion by ATP-dependent chromatin remodeling activities. *Cell*, **103**, 1133–1142.
13. Flaus,A. and Owen-Hughes,T. (2004) Mechanisms for ATP-dependent chromatin remodelling: farewell to the tuna-can octamer? *Curr. Opin. Genet. Dev.*, **14**, 165–173.
14. Redd,M.J., Arnaud,M.B. and Johnson,A.D. (1997) A complex composed of tup1 and ssn6 represses transcription in vitro. *J. Biol. Chem.*, **272**, 11193–11197.
15. Cooper,J.P., Roth,S.Y. and Simpson,R.T. (1994) The global transcriptional regulators, SSN6 and TUP1, play distinct roles in the establishment of a repressive chromatin structure. *Genes Dev.*, **8**, 1400–1410.
16. Davie,J.K., Trumbly,R.J. and Dent,S.Y. (2002) Histone-dependent association of Tup1-Ssn6 with repressed genes in vivo. *Mol. Cell. Biol.*, **22**, 693–703.
17. Bone,J.R. and Roth,S.Y. (2001) Corepressor proteins and control of transcription in yeast. *Curr. Top. Microbiol. Immunol.*, **254**, 59–78.
18. Davie,J.K., Edmondson,D.G., Coco,C.B. and Dent,S.Y. (2003) Tup1-Ssn6 interacts with multiple class I histone deacetylases in vivo. *J. Biol. Chem.*, **278**, 50158–50162.
19. Wu,J., Suka,N., Carlson,M. and Grunstein,M. (2001) TUP1 utilizes histone H3/H2B-specific HDA1 deacetylase to repress gene activity in yeast. *Mol. Cell*, **7**, 117–126.
20. Malave,T.M. and Dent,S.Y. (2006) Transcriptional repression by Tup1-Ssn6. *Biochem. Cell Biol.*, **84**, 437–443.
21. Fleming,A.B. and Pennings,S. (2001) Antagonistic remodelling by Swi-Snf and Tup1-Ssn6 of an extensive chromatin region forms the background for *FLO1* gene regulation. *EMBO J.*, **20**, 5219–5231.
22. Gavin,I.M. and Simpson,R.T. (1997) Interplay of yeast global transcriptional regulators Ssn6p-Tup1p and Swi-Snf and their effect on chromatin structure. *EMBO J.*, **16**, 6263–6271.
23. Sharma,V.M., Li,B. and Reese,J.C. (2003) SWI/SNF-dependent chromatin remodeling of RNR3 requires TAF(II)s and the general transcription machinery. *Genes Dev.*, **17**, 502–515.
24. Almer,A., Rudolph,H., Hinnen,A. and Hörz,W. (1986) Removal of positioned nucleosomes from the yeast *PHO5* promoter upon *PHO5* induction releases additional upstream activating DNA elements. *EMBO J.*, **5**, 2689–2696.
25. Moreira,J.M. and Holmberg,S. (1998) Nucleosome structure of the yeast *CHA1* promoter: analysis of activation-dependent chromatin remodeling of an RNA-polymerase-II-transcribed gene in TBP and RNA pol II mutants defective in vivo in response to acidic activators. *EMBO J.*, **17**, 6028–6038.
26. Verdone,L., Camilloni,G., Di Mauro,E. and Caserta,M. (1996) Chromatin remodeling during *Saccharomyces cerevisiae ADH2* gene activation. *Mol. Cell. Biol.*, **16**, 1978–1988.
27. Zhang,Z. and Reese,J.C. (2004) Redundant mechanisms are used by Ssn6-Tup1 in repressing chromosomal gene transcription in Saccharomyces cerevisiae. *J. Biol. Chem.*, **279**, 39240–39250.
28. Kim,Y. and Clark,D.J. (2002) SWI/SNF-dependent long-range remodeling of yeast *HIS3* chromatin. *Proc. Natl Acad. Sci. USA*, **99**, 15381–15386.
29. Kim,Y., McLaughlin,N., Lindstrom,K., Tsukiyama,T. and Clark,D.J. (2006) Activation of Yeast *HIS3* results in Gcn4p-dependent, SWI/SNF-dependent mobilization of nucleosomes over the entire gene. *Mol. Cell. Biol.*, **26**, 8607–8622.
30. Shen,C.H. and Clark,D.J. (2001) DNA sequence plays a major role in determining nucleosome positions in yeast *CUP1* chromatin. *J. Biol. Chem.*, **276**, 35209–35216.
31. Carlson,M. and Botstein,D. (1982) Two differentially regulated mRNAs with different 5' ends encode secreted with intracellular forms of yeast invertase. *Cell*, **28**, 145–154.
32. Trumbly,R.J. (1992) Glucose repression in the yeast Saccharomyces cerevisiae. *Mol. Microbiol.*, **6**, 15–21.
33. Carlson,M., Osmond,B.C., Neigeborn,L. and Botstein,D. (1984) A suppressor of SNF1 mutations causes constitutive high-level invertase synthesis in yeast. *Genetics*, **107**, 19–32.
34. Williams,F.E. and Trumbly,R.J. (1990) Characterization of TUP1, a mediator of glucose repression in Saccharomyces cerevisiae. *Mol. Cell. Biol.*, **10**, 6500–6511.
35. Vallier,L.G. and Carlson,M. (1994) Synergistic release from glucose repression by mig1 and ssn mutations in Saccharomyces cerevisiae. *Genetics*, **137**, 49–54.
36. Carlson,M. and Botstein,D. (1983) Organization of the *SUC* gene family in Saccharomyces. *Mol. Cell. Biol.*, **3**, 351–359.
37. Gregory,P.D. and Hörz,W. (1999) Mapping chromatin structure in yeast. *Methods Enzymol.*, **304**, 365–376.
38. Perez-Ortin,J.E., Estruch,F., Matallana,E. and Franco,L. (1986) DNase I sensitivity of the chromatin of the yeast SUC2 gene for invertase. *Mol. Gen. Genet.*, **205**, 422–427.
39. Perez-Ortin,J.E., Estruch,F., Matallana,E. and Franco,L. (1987) Fine analysis of the chromatin structure of the yeast *SUC2* gene and of its changes upon derepression. Comparison between the chromosomal and plasmid-inserted genes. *Nucleic Acids Res.*, **15**, 6937–6956.
40. Matallana,E., Franco,L. and Perez-Ortin,J.E. (1992) Chromatin structure of the yeast *SUC2* promoter in regulatory mutants. *Mol. Gen. Genet.*, **231**, 395–400.
41. Hirschhorn,J.N., Brown,S.A., Clark,C.D. and Winston,F. (1992) Evidence that SNF2/SWI2 and SNF5 activate transcription in yeast by altering chromatin structure. *Genes Dev.*, **6**, 2288–2298.
42. Hirschhorn,J.N., Bortvin,A.L., Ricupero-Hovasse,S.L. and Winston,F. (1995) A new class of histone H2A mutations in Saccharomyces cerevisiae causes specific transcriptional defects in vivo. *Mol. Cell. Biol.*, **15**, 1999–2009.
43. Wu,L. and Winston,F. (1997) Evidence that Snf-Swi controls chromatin structure over both the TATA and UAS regions of the *SUC2* promoter in Saccharomyces cerevisiae. *Nucleic Acids Res.*, **25**, 4230–4234.
44. Carlson,M. (1999) Glucose repression in yeast. *Curr. Opin. Microbiol.*, **2**, 202–207.
45. Zhou,H. and Winston,F. (2001) NRG1 is required for glucose repression of the *SUC2* and *GAL* genes of *Saccharomyces cerevisiae*. *BMC Genet.*, **2**, 1471–2156.
46. Buck,M.J. and Lieb,J.D. (2006) A chromatin-mediated mechanism for specification of conditional transcription factor targets. *Nat. Genet.*, **38**, 1446–1451.
47. Adkins,M.W. and Tyler,J.K. (2006) Transcriptional activators are dispensable for transcription in the absence of Spt6-mediated chromatin reassembly of promoter regions. *Mol. Cell*, **21**, 405–416.
48. Sekinger,E.A., Moqtaderi,Z. and Struhl,K. (2005) Intrinsic histone-DNA interactions and low nucleosome density are important for preferential accessibility of promoter regions in yeast. *Mol. Cell*, **18**, 735–748.
49. Papamichos-Chronakis,M., Petrakis,T., Ktistaki,E., Topalidou,I. and Tzamarias,D. (2002) Cti6, a PHD domain protein, bridges the Cyc8-Tup1 corepressor and the SAGA coactivator to overcome repression at *GAL1*. *Mol. Cell*, **9**, 1297–1305.
50. Segal,E., Fondufe-Mittendorf,Y., Chen,L., Thastrom,A., Field,Y., Moore,I.K., Wang,J.P. and Widom,J. (2006) A genomic code for nucleosome positioning. *Nature*, **442**, 772–778.
51. Kelbauskas,L., Chan,N., Bash,R., Yodh,J., Woodbury,N. and Lohr,D. (2007) Sequence-dependent nucleosome structure and

stability variations detected by forster resonance energy transfer. *Biochemistry*, **46**, 2239–2248.
52. Bash,R.C., Vargason,J.M., Cornejo,S., Ho,P.S. and Lohr,D. (2001) Intrinsically bent DNA in the promoter regions of the yeast *GAL1-10* and *GAL80* genes. *J. Biol. Chem.*, **276**, 861–866.
53. Iyer,V.R., Horak,C.E., Scafe,C.S., Botstein,D., Snyder,M. and Brown,P.O. (2001) Genomic binding sites of the yeast cell-cycle transcription factors SBF and MBF. *Nature*, **409**, 533–538.
54. Lieb,J.D., Liu,X., Botstein,D. and Brown,P.O. (2001) Promoter-specific binding of Rap1 revealed by genome-wide maps of protein-DNA association. *Nat. Genet.*, **28**, 327–334.
55. Mennella,T.A., Klinkenberg,L.G. and Zitomer,R.S. (2003) Recruitment of Tup1-Ssn6 by yeast hypoxic genes and chromatin-independent exclusion of TATA binding protein. *Eukaryot. Cell*, **2**, 1288–1303.
56. Valenzuela,L. and Kamakaka,R.T. (2006) Chromatin Insulators. *Annu. Rev. Genet.*, **40**, 107–138.
57. Donze,D. and Kamakaka,R.T. (2001) RNA polymerase III and RNA polymerase II promoter complexes are heterochromatin barriers in *Saccharomyces cerevisiae*. *EMBO J.*, **20**, 520–531.
58. Ferrari,S., Simmen,K.C., Dusserre,Y., Muller,K., Fourel,G., Gilson,E. and Mermod,N. (2004) Chromatin domain boundaries delimited by a histone-binding protein in yeast. *J. Biol. Chem.*, **279**, 55520–55530.
59. Boukaba,A., Georgieva,E.I., Myers,F.A., Thorne,A.W., Lopez-Rodas,G., Crane-Robinson,C. and Franco,L. (2004) A short-range gradient of histone H3 acetylation and Tup1p redistribution at the promoter of the Saccharomyces cerevisiae *SUC2* gene. *J. Biol. Chem.*, **279**, 7678–7684.
60. Geng,F. and Laurent,B.C. (2004) Roles of SWI/SNF and HATs throughout the dynamic transcription of a yeast glucose-repressible gene. *EMBO J.*, **23**, 127–137.
61. Bazett-Jones,D.P., Côté,J., Landel,C.C., Peterson,C.L. and Workman,J.L. (1999) The SWI/SNF complex creates loop domains in DNA and polynucleosome arrays and can disrupt DNA-histone contacts within these domains. *Mol. Cell. Biol.*, **19**, 1470–1478.
62. Gavin,I., Horn,P.J. and Peterson,C.L. (2001) SWI/SNF chromatin remodeling requires changes in DNA topology. *Mol. Cell*, **7**, 97–104.
63. Ducker,C.E. and Simpson,R.T. (2000) The organized chromatin domain of the repressed yeast a cell-specific gene *STE6* contains two molecules of the corepressor Tup1p per nucleosome. *EMBO J.*, **19**, 400–409.
64. Horn,P.J., Crowley,K.A., Carruthers,L.M., Hansen,J.C. and Peterson,C.L. (2002) The SIN domain of the histone octamer is essential for intramolecular folding of nucleosomal arrays. *Nat. Struct. Biol.*, **9**, 167–171.
65. Sarma,N.J., Haley,T.M., Barbara,K.E, Buford,T.D., Willis,K.A. and Santangelo,G.M. (2007) Glucose-responsive regulators of gene expression in *Saccharomyces cerevisiae* function at the nuclear periphery via a reverse recruitment mechanism. *Genetics*, **175**, 1127–1135.
66. Millar,C.B. and Grunstein,M. (2006) Genome-wide patterns of histone modifications in yeast. *Nat. Rev. Mol. Cell Biol.*, **7**, 657–666.